Journal of Alloys and Compounds, 182 (1992) 271–280
JALCOM 156

Experimental study of the Al–Cr equilibrium diagram

Joaquim G. Costa Neto, Sergio Gama and Carlos A. Ribeiro
Instituto de Física Gleb Wataghin, Universidade Estadual de Campinas, UNICAMP
C.P. 6165, CEP 13081, Campinas, SP (Brazil)

(Received September 24, 1991; in final form October 21, 1991)

Abstract

The phase diagram for the Al–Cr system has been experimentally revised. The main features of the diagram in the literature have been confirmed. The γ ($Al_{11}Cr_2$) phase has not been found in as-cast samples, heat-treated samples or samples subjected to differential thermal analysis. A diffusion couple treated at 650 °C has not shown this phase either. The reaction involving the aluminium phase has been found to be of a eutectic nature. A new version of the Al–Cr phase diagram is proposed, taking account of these findings and literature data.

1. Introduction

The Al–Cr phase diagram has been extensively studied. The first consistent version is from Bradley and Lu [1], based on their own measurements and on previous measurements from Goto and Dogane [2] and Fink and Freche [3]. Zoller redetermined the chromium solubility in aluminium [4]; Köster *et al.* [5] redetermined the diagram completely using metallography, X-ray diffraction analyses and magnetic susceptibility measurements. This work has been reproduced in a recent critical evaluation of the binary diagram [6]. Figure 1 presents this version of the Al–Cr system.

The data of Köster *et al.* show the existence of six intermetallic compounds, five of them forming peritectically. The β phase has the stoichiometry Al_7Cr, the γ phase is $Al_{11}Cr_2$, the δ phase is Al_4Cr, the ϵ phase has the general stoichiometry Al_9Cr_4 and presents three modifications designated ϵ_1, ϵ_2 and ϵ_3, the ζ phase is Al_8Cr_5 and presents two modifications designated ζ_1 and ζ_2, and finally the η phase has the composition $AlCr_2$, being an ordered superstructure of the b.c.c. solid solution of aluminium in chromium. Most authors describe a peritectic reaction of formation for aluminium solid solution (Al) at 661 °C [1, 3, 6], while Goto and Dogane [2] suggested a eutectic reaction between (Al) and the β phase.

The activity of aluminium in solid Al–Cr alloys has been measured by an isopiestic technique between 890 and 1126 °C and concentrations from 13 to 80 at.% Al. The maximum solid solubility of aluminium in chromium was confirmed to be 43 at.% Al at 1000 °C, and the solubility limits at 1000 °C were determined as from 20 to 21 at.% Cr for δ phase, from 30

0925-8388/92/$5.00

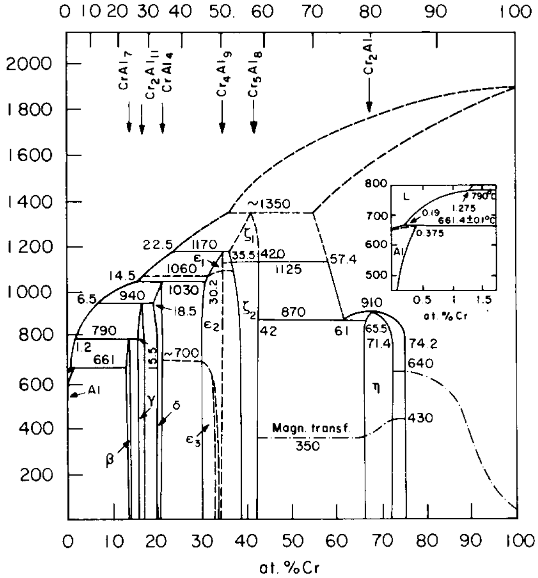

Fig. 1. The Al–Cr phase diagram after Köster *et al.* [5] and Massalski [6].

to 34 at.% Cr for the ϵ phase and from 37 to 41 at.% Cr for the ζ phase [7].

Tendeloo *et al.* [8] and den Broeder *et al.* [9] did metallographic, X-ray diffraction and high resolution microscopic analyses of alloys in the chromium-rich region of the phase diagram. They pointed out the possible existence of a new phase, designated as X phase, that can be described either as a rhombohedral Al_3Cr_5 or $AlCr_3$ superlattice, or as a concentration modulation of the chromium solid solution. This new phase should be formed peritectoidally at low temperatures (around 400 °C) and have an estimated existence range from 75 to 80 at.% Cr.

Recently, Ellner *et al.* [10] did metallographic and X-ray diffraction analyses of Al–Cr alloys in the composition interval from 30 to 100 at.% Cr, using heat-treated as well as rapidly quenched samples. They confirmed the magnetic ordering of the η phase through the temperature dependence of the lattice parameters. The dependence of the lattice parameters of the ζ phase on aluminium concentration has also been measured and they confirmed the existence of the ϵ_2 and ϵ_3 modifications, as well as the translation group of the ϵ_3 modification. The rapidly quenched samples in the composition interval from 30 to 42 at.% Cr showed a new phase isotypic with Cu_5Zn_8.

The aim of this work is an experimental revision of the Al–Cr phase diagram, as part of a more general study of the ternary system Al–Cr–Nb. Some discrepancies were found between our findings and the accepted phase diagram, and these motivated the present paper.

2. Experimental procedure

The starting materials for alloy preparation were 99.5% chromium powder from Fluka and 99.9% aluminium rods from Alcoa. Samples were melted at least three times in an arc furnace under a high purity argon atmosphere, being turned between meltings for better homogenization. Weight losses were negligible. For the heat treatments the samples were sealed in quartz ampoules with high purity argon.

Pieces of the as-cast and heat-treated samples were metallographically analysed using standard procedures, final polishing being attained with 1 μm diamond paste. Etching was carried out with a solution of sol H_2O–HNO_3–HF (10:5:1 in volume), with etching times increasing from 5 to 30 s as the chromium content increased. Photomicrographs were obtained in a Neophot-32 Zeiss metallograph. Vickers microhardness measurements were done in the same microscope using a special attachment. Differential thermal analyses (DTAs) were carried out up to 1550 °C in a Netzsch apparatus, with the samples in alumina crucibles and submitted to two heating–cooling cycles, the first at 10 °C min^{-1} and the second at 5 °C min^{-1}. Electron microprobe measurements in metallographically prepared samples were done in a Camebax scanning electron microscope.

3. Results and discussion

The analysis of the Al–Cr system began by verifying the existence of all phases and the nature of the reactions occurring in the diagram. The analyses of samples in the chromium-rich part of the diagram confirmed the aluminium solubility range, the congruent formation of the ordered phase η ($AlCr_2$), the peritectic formation of the ζ (Al_8Cr_5) phase and the eutectoid reaction between η and ζ. Figure 2 shows the micrography of the as-cast Al–55%Cr alloy (all concentrations in this work are expressed in atoms per cent). We can observe the primary precipitation of the chromium solid solution

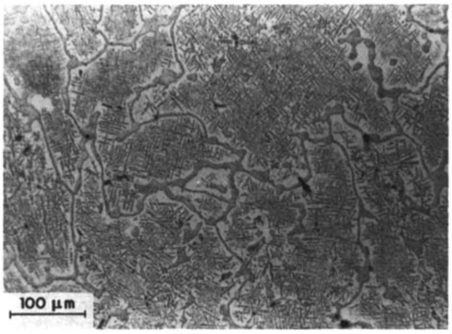

Fig. 2. Micrography of the as-cast Al–55%Cr alloy, showing (Cr) grains that decomposed eutectoidly in ζ and η, surrounded by dark grey ζ phase.

(Cr), the peritectic layers of ζ surrounding the (Cr) grains and the eutectoid decomposition of (Cr) into ζ and η. Our DTA measurements for this alloy show the eutectoid temperature as 872 °C (Table 1), in very good agreement with the literature [5, 6]. The DTA measurements for the 40 and 44% Cr show the peritectic reaction of formation of ζ occurring at 1315 °C, instead of 1350 °C [5, 6]. Also the temperature for the transformation $\zeta_1 \rightleftharpoons \zeta_2$ has been measured as 1115 °C, very near the literature value of 1125 °C [5, 6]. Our DTA apparatus had insufficient sensitivity to detect the ordering transformation $(Cr) \rightleftharpoons \eta$.

Figure 3 shows the micrography of the Al–40%Cr alloy heat treated at 870 °C for 360 h. It is single phase and presents twinning indicating the $\zeta_1 \rightleftharpoons \zeta_2$ transformation.

Our observations also confirm the peritectic formation of the ϵ (Al_9Cr_4) phase. Figure 4 shows the micrography of Al–31%Cr heat treated at 650 °C for 450 h. It is also single phase, the dark regions being pores, probably coming from a Kirkendall-like phenomenon. DTA measurements confirm the peritectic reaction occurring at 1165 °C (Table 1), also in good agreement with the literature data [5, 6]. The $\epsilon_1 \rightleftharpoons \epsilon_2$ transformation has been detected as occurring at 1065 °C.

The peritectic formation of the δ (Al_4Cr) phase is confirmed. Figure 5 shows the microstructure of the Al–20.5%Cr DTA sample, submitted to a final cooling rate of 5 °C min^{-1} in the DTA apparatus. The dark phase in the central part of the grains is primarily precipitated ϵ, surrounded by peritectic δ. The white phase is β (Al_7Cr). The compositions were confirmed by electron microprobe measurements. Our DTA data indicate the δ peritectic reaction temperature to be 1035 °C, also in good agreement with the literature [5, 6].

Analyses of aluminium-rich alloys in the composition interval from 12.5 to 20% Cr failed to show up the existence of the γ ($Al_{11}Cr_2$) phase. For all analysed alloys only the δ and β phases were detected. Figure 6 shows the micrography of the Al–13.5%Cr alloy in the as-cast state. The primary precipitates (dark grey) correspond to the δ phase surrounded by a thick layer of β (light grey). The white phase is (Al.). Our DTA measurements do not show any peak or signal at 940 °C, which is indicated in the literature as the γ formation temperature. Figure 7 shows the microstructure of Al–15%Cr heat treated at 650 °C for 450 h. The dark grey phase is δ and the lighter one is β, while the dark regions correspond to pores. There is no indication of γ stabilization. The compositions of the phases have been confirmed by microprobe measurements.

Figure 8 shows the micrography of the Al–6.5%Cr alloy, measured in the DTA apparatus, that had been submitted to a final cooling rate of 5 °C min^{-1}. The dark grey phase in the centre of the grains is the δ phase, surrounded by a thick layer of the lighter grey β phase. Finally, the white phase corresponds to (Al). This microstructure clearly shows the peritectic nature of the β phase. The DTA data show this peritectic temperature as 835 °C, instead of 790 °C as in the literature [5, 6]. Most samples in this

TABLE 1

DTA results for the alloys studied

Reaction	Results for various Al–Cr samples											
	5.5^{a}	6.5	12.0	16.0	18.0	20.5	32.5	37.0	40.0	44.0	55.5	61.0
$L+\beta \rightleftarrows Al$	658–657^{b}	655–655^{b}	656–658^{b}	657–657^{b}	–	655–655^{b}	–	–	–	–	–	–
$L+\delta \rightleftarrows \beta$	840–770^{b}	831–761^{b}	829–778^{b}	839–783^{b}	785^{c}	770^{c}	–	–	–	–	–	–
$L+\epsilon_2 \rightleftarrows \delta$	–	–		1033–984^{b}	1035–999^{b}	1032–985^{b}	1035–1035^{b}	1035–1035^{b}	–	–	–	–
$\epsilon_1 \rightleftarrows \epsilon_2$	–	–	–	–	–	–	–	1070^{c}	–	1064^{d}	1065^{d}	–
$\zeta_1 \rightleftarrows \zeta_2$	–	–	–	–	–	–	–	–	1115–1101^{b}	1124–1111^{b}	–	–
$L+\zeta_1 \rightleftarrows \epsilon_1$	–	–	–	–	–	–	1164^{c}	–	–	–	–	–
$L+Cr \rightleftarrows \zeta_1$	–	–	–	–	–	–	–	–	1311^{c}	1312–1318^{b}	–	–
$Cr \rightleftarrows \eta$	–	–	–	–	–	–	–	–	–	–	–	–
$\zeta_2+\eta \rightleftarrows Cr$	–	–	–	–	–	–	–	–	–	–	872–857^{b}	872–825^{b}
Liquidus curve	902^{c}	918^{c}	970–963^{b}	1041^{c}	1125–1125^{b}	1129^{c}	1267–1273^{b}	–	–	–	–	–

[a] Chromium content (at.%).

[b] Temperatures for the heating–cooling parts of the cycles (°C).

[c] Temperature for the cooling part of the cycle (°C).

[d] Temperature for the heating part of the cycle (°C).

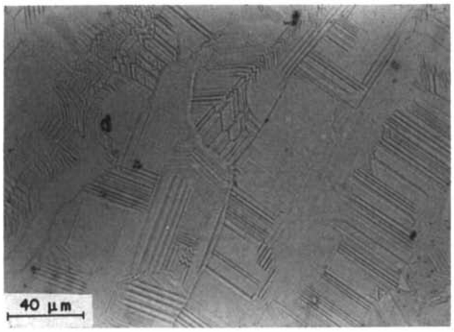

Fig. 3 Micrography of the Al–40%Cr alloy heat treated at 870 °C for 360 h. Note twinning due to the $\zeta_1 \rightleftharpoons \zeta_2$ transformation.

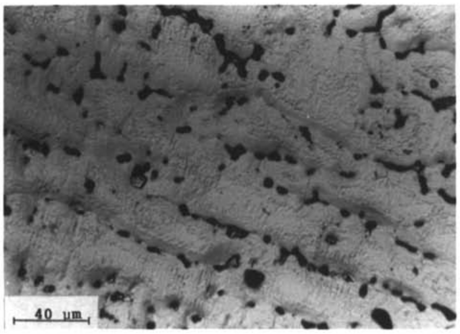

Fig. 4. Micrography of the Al–31%Cr heat treated at 650 °C for 450 h (single-phase ϵ_2).

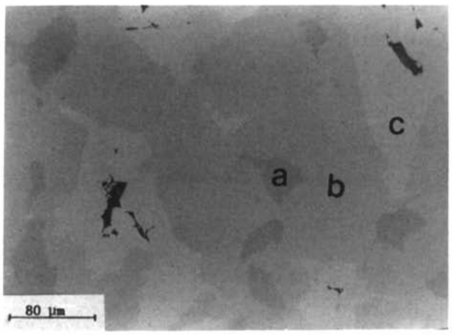

Fig. 5. Micrography of the Al–20.5%Cr DTA sample. The dark grey area (a) is the primary ϵ phase, the light grey area (b) is the δ phase and the white area (c) is β.

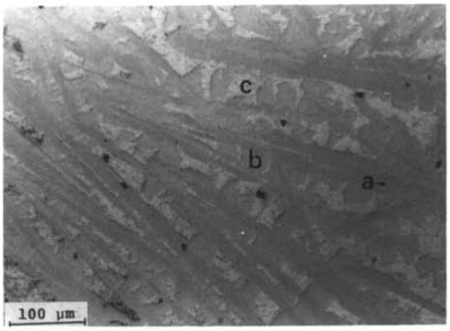

Fig. 6. Micrography of the as-cast Al–13.5%Cr. The dark grey area (a) is the δ phase, surrounded by the β phase (b). The white regions (c) are (Al).

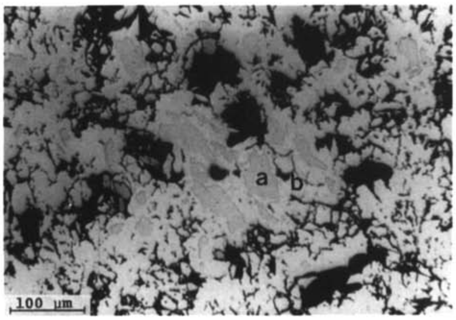

Fig. 7. Micrography of the Al–15%Cr alloy heat treated at 650 °C for 450 h. The light grey phase (a) is δ, the white phase (b) is β. Black areas are pores.

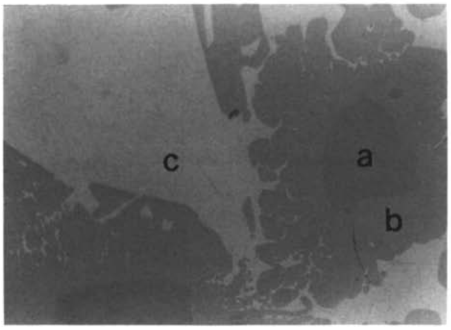

Fig. 8. Micrography of the Al–6.5%Cr DTA sample. The dark grey phase (a) is the primary δ phase, surrounded by the (light grey) β phase (b). The white phase (c) is (Al).

aluminium-rich region show great undercoolings relative to this peritectic reaction (see Table 1), with a big thermal signal around 770 °C. The value of 835 °C attributed to this reaction is the averaged value obtained in the several DTA heating cycles.

Alloys that are aluminium rich, as 6.5% Cr, as cast or heat treated at 650 °C for 450 h, show only the β and (Al) phases. The heat-treated sample shows β as polyhedral-shaped grains (Fig. 9). The DTA analyses of these samples, and of others up to 20.5% Cr, consistently show the temperature of the reaction involving β and (Al) to be 657 °C, below the aluminium melting point (Table 1). This strongly suggests that this reaction is not peritectic, but eutectic, as first pointed out by Goto and Dogane [2]. Figure 8 does not display a typical eutectic microstructure for the white phase, because the eutectic composition is very close to (Al).

To complement the study of the Al–Cr phase diagram, a diffusion couple has been utilized. A chromium crucible was constructed with a conical lid, and aluminium pieces were put inside it. To close the crucible, the conical lid has been pressed into the crucible. After that, the set was encapsulated in a quartz ampoule with high purity argon. Before the heat treatment, the furnace was heated to 700 °C for 30 min in order to melt the aluminium, then the temperature was lowered to 630 °C and maintained at this level for 170 h. Figure 10 shows the resulting micrography. Five layers were formed, and their compositions were determined by electron microprobe measurements. Surprisingly, these measurements showed a composition corresponding to the γ phase (16.8% Cr) and a second one of 25.6% Cr. These stoichiometries have no correspondence to the phases observed in any as-cast, heat-treated or DTA alloy of this work. One possible explanation for the appearance of these two new phases is the probable contamination of the diffusion couple by oxygen and nitrogen, once the aluminium pieces

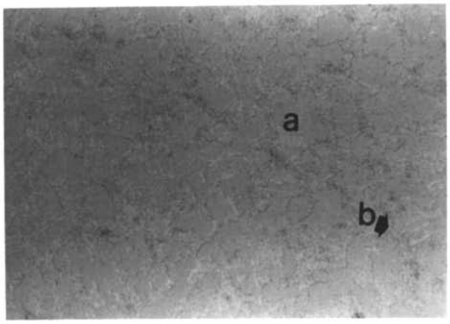

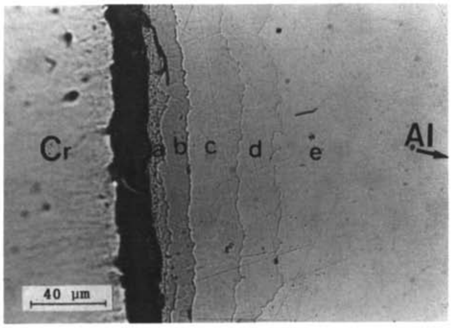

Fig. 9. Micrography of the Al–6.5%Cr alloy heat treated at 650 °C for 450 h. Note the polyhedral-shaped β phase (a) grains in the (Al) matrix (b).

Fig. 10. Al–Cr diffusion couple heat treated at 630 °C for 170 h. Electron microprobe analysis indicates the following compositions for the layers: a, 31.6% Cr; b, 25.6% Cr; c, 19.5% Cr; d, 16.8% Cr; e, 13.8% Cr.

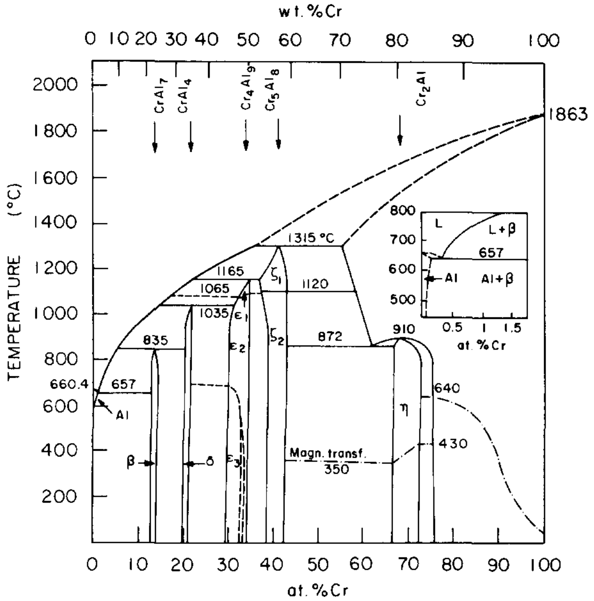

Fig. 11. The Al–Cr phase diagram according to the present work and pertinent literature data.

were closed inside the chromium crucible in the presence of air. More work is being done in order to clarify this point.

Figure 11 shows the Al–Cr phase diagram according to our data and the pertinent literature data [5, 6]. The insert shows the aluminium-rich side of the diagram, with the eutectic reaction between (Al) and β. The literature [6] about the aluminium phase diagrams with the transition metals (nickel, cobalt, iron, manganese, chromium, vanadium, titanium) shows that from nickel up to manganese the aluminium-rich side presents a eutectic reaction, and that vanadium and titanium show a peritectic reaction. It is apparent that chromium is at the point where the nature of the reaction changes from one type to the other.

Vickers microhardness measurements were performed for the whole composition range. They are presented in Fig. 12 and in Table 2, where they are compared with available literature data [11, 12]. The values for aluminium and the β phase are in good agreement with the literature [11], while our value for chromium is significantly higher than the literature value [12].

4. Conclusions

The Al–Cr phase diagram has been revised. The main points to be stressed are as follows.

The aluminium solubility in chromium has been confirmed, as well as the eutectoid reaction between the ζ_2 (Al_8Cr_5) and η ($AlCr_2$) phases.

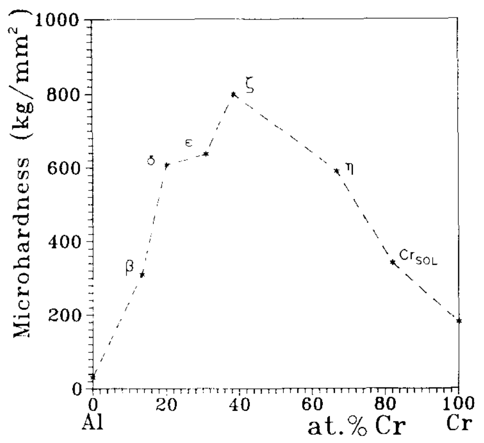

Fig. 12. Vickers microhardness measurements for the Al–Cr alloys.

TABLE 2

Vickers microhardness results (kgf mm^{-2}) for the Al–Cr alloys

Phase	Literature results		Results of this work	
	Value	Load (gf)	Value	Load (gf)
Al	10–35[a]	–	30±5	5
β	310±80[b]	20	309±30	10
γ	650±40[b]	20	–	–
δ	–	–	608±60	15
ϵ_2	–	–	637±70	20
ζ_2	–	–	800±80	20
η	–	–	590±50	15
(Cr)	–	–	340±30	15
Cr	70–110	–	180±30	10

[a] From ref. 11.
[b] From ref. 12.

The peritectic formation of the ζ_1, ϵ_1, δ and β phases as well as their peritectic temperatures have been confirmed.

The γ ($Al_{11}Cr_2$) phase was not confirmed in the as-cast, heat-treated or DTA samples.

The reaction involving (Al) and β (Al_7Cr) is of a eutectic nature, with a temperature of 657 °C.

Acknowledgments

We acknowledge financial support from Fundação de Amparo à Pesquisa do Estado de São Paulo, Centro de Materiais Refratários da Fundação de

Tecnologia Industrial, Lorena, SP, and Conselho Nacional de Pequisa e Desenvolvimento Tecnológico.

References

1 A. J. Bradley and S. S. Lu, *J. Inst. Met.*, *60* (1937) 319–337.

2 M. Goto and G. Dogane, *Nippon Kogyo Kaishi*, *43* (1927) 931; *J. Inst. Met.*, *43* (1930) 446.

3 W. L. Fink and H. R. Freche, *Trans. Metall. Soc. AIME*, *104* (1933) 325–334.

4 H. Zoller, *Schweiz. Arch. Angew. Wiss. Tech.*, *26* (1960) 437–448.

5 W. Köster, E. Wachtel and K. Grube, *Z. Metallkde.*, *54* (1963) 7, 393–401.

6 T. B. Massalski (ed.), *Binary Alloy Phase Diagrams*, Vol. I, American Society for Metals, Metals Park, OH, 1986, p. 103.

7 W. Johnson, K. Komarek and E. Miller, *Trans. Metall. Soc. AIME*, *242* (1968) 1685–1688.

8 G. van Tendeloo, F. J. A. den Broeder, A. Amelinckx, R. de Ridder, J. van Landuyt and H. J. van Daal, *Phys. Status Solidi A*, *67* (1981) 217–232.

9 F. J. A. den Broeder, G. van Tendeloo, S. Amelinckx, J. Hornstra, R. de Ridder, J. van Landuyt and H. J. van Daal, *Phys. Status Solidi A*, *67* (1981) 233–248.

10 M. Ellner, J. Braun and B. Predel, *Z. Metallkde.*, *80* (1989) 5, 374–385.

11 R. D. Vengrenovich and V. I. Psarev, *Fiz. Met. Metalloved.*, *29* (1970) 3, 540.

12 *Metals Handbook*, Vol. 2, 8th edn., American Society for Metals, Metals Park, OH, 1975, p. 292.